Induced-fit tightens pleuromutilins binding to ribosomes and remote interactions enable their selectivity

Chen Davidovich*, Anat Bashan*, Tamar Auerbach-Nevo*, Rachel D. Yaggie†, Richard R. Gontarek†, and Ada Yonath*‡

*Department of Structural Biology, Weizmann Institute, Rehovot 76100, Israel; and †Department of Enzymology and Mechanistic Pharmacology, GlaxoSmithKline, 1250 South Collegeville Road, Collegeville, PA 19426

Contributed by Ada Yonath, January 3, 2007 (sent for review December 4, 2006)

New insights into functional flexibility at the peptidyl transferase center (PTC) and its vicinity were obtained by analysis of pleuromutilins binding modes to the ribosome. The crystal structures of *Deinococcus radiodurans* large ribosomal subunit complexed with each of three pleuromutilin derivatives: retapamulin (SB-275833), SB-280080, and SB-571519, show that all bind to the PTC with their core oriented similarly at the A-site and their C14 extensions pointing toward the P-site. Except for an H-bond network with a single nucleotide, G2061, which involves the essential keto group of all three compounds, only minor hydrophobic contacts are formed between the pleuromutilin C14 extensions and any ribosomal component, consistent with the PTC tolerance to amino acid diversity. Efficient drug binding mode is attained by a mechanism based on induced-fit motions exploiting the ribosomal intrinsic functional flexibility and resulting in conformational rearrangements that seal the pleuromutilin-binding pocket and tightens it up. Comparative studies identified a network of remote interactions around the PTC, indicating that pleuromutilins selectivity is acquired by nonconserved nucleotides residing in the PTC vicinity, in a fashion resembling allosterism. Likewise, pleuromutilin resistant mechanisms involve nucleotides residing in the environs of the binding pocket, consistent with their slow resistance-development rates.

antibiotics | functional flexibility | ribosome crystallography | peptidyl transferase center | retapamulin

As a result of the dramatic increase in antibiotic resistance among pathogenic bacterial strains, which now represents a significant health threat (1), the arsenal of efficient antibacterial drugs is being depleted. A promising strategy for alleviating this problem is the introduction of antibiotics from classes that have a unique mode of action. Owing to the critical role of ribosomes in cell vitality, various clinically relevant antibiotics target its functional sites. Although most of these sites are highly conserved, some of them consist of a single or a few elements that underwent evolutionary diversity, and thus enable the distinction between pathogenic and eukaryotic ribosomes, a major factor in facilitating their clinical use. Position 2058 in the macrolide binding pocket (adenine in eubacteria, guanine in eukaryotes) is an example for a rRNA sequence divergence that is used as an efficient tool for antibiotics selectivity, as well as for genetic or chemical modifications acquiring resistance. The peptidyl transferase center (PTC), however, is almost fully conserved across all kingdoms of life, yet hosting several families of antibiotics, among them are the pleuromutilins that selectively target the bacterial ribosome with a slow development of resistance.

Pleuromutilin is a natural product of the fungi *Pleurotus mutilus* (now called *Clitopilus scyphoides*) (2) (Fig. 1), which was used as a base for a class of antibacterial agents (3), designed for clinical utilization by targeting eubacterial ribosomes. They consists of a common tricyclic mutilin core, a C21 keto group, essential for antimicrobial activity (3) and various substituents at its C14, most of which are extensions of diverse chemical nature. During the early 1980s, extensive effort was made to formulate azamulin (Fig. 1) for clinical use in human (4, §, ¶, ‖) because it is active against many clinical isolates, including erythromycin and tetracycline-resistant strains. However, because it strongly inhibits cytochrome P450**, it never progressed beyond phase I clinical trials.†† Continuous efforts to develop pleuromutilin antibiotics yielded several semisynthetic derivatives, some of which with elevated activity over a broad spectrum of pathogens. The most advanced compound, retapamulin (SB-275833; SmithKline Beecham), has potent activity against Gram-positive pathogens (5–11) and a low propensity to select for resistance (12), has recently completed phase III clinical trials as a topical agent, showing that all strains of *Staphylococcus aureus* and *Streptococcus pyogenes* were susceptible to retapamulin with MICs ≤ 0.5 μg/ml (13, 14).

Retapamulin and SB-280080 (Fig. 1) are C14-sulfanyl-acetate derivatives of pleuromutilin. This group, which includes also tiamulin, valnemulin, and azamulin, is characterized by a broad-spectrum activity against various clinically relevant bacterial strains (8, 15) but limited oral bioavailability (15, 16). However, the C14-acyl-carbamate derivatives, which include SB-571519 (Fig. 1), undergo reduced metabolism (16), thus more suitable for oral administration. As observed biochemically, pleuromutilins interfere with peptide bond formation (17–21). Consistently, the only available crystal structure of a pleuromutilin antibiotic, tiamulin, bound to the large ribosomal subunit verifies binding to the PTC (22).

Here, we present the crystal structures of complexes of the large ribosomal subunit of the model pathogen *Deinococcus radiodurans* (D50S) with three pleuromutilin derivatives, SB-275833, SB-280080, and SB-571519, which represent the two groups of the semisynthetic pleuromutilins described above. Thorough compar-

BIOCHEMISTRY

Author contributions: C.D., A.B., R.R.G., and A.Y. designed research; C.D., A.B., T.A.-N., and R.D.Y. performed research; T.A.-N. contributed new reagents/analytic tools; C.D., A.B., and A.Y. analyzed data; and C.D., A.B., and A.Y. wrote the paper.

Conflict of interest: R.R.G. is an employee and shareholder of GlaxoSmithKline; R.D.Y. is an employee of GlaxoSmithKline.

Freely available online through the PNAS open access option.

Abbreviation: PTC, peptidyl transferase center.

‡To whom correspondence should be addressed. E-mail: ada.yonath@weizmann.ac.il.

§Hildebrandt, J., Berner, H., Laber, G., Schuetze, E., Turnowsky, F. (1983) in *Proceedings of the 13th Internal Congress of Chemotherapy*, eds. Spitzy, K., Karrer, K. (H. Egermann, Vienna), Vol. 5, pp. 108/124–108/128 (abstr.).

¶Hoegenauer, G., Brunowsky, W. (1983) in *Proceedings of the 13th Internal Congress of Chemotherapy*, eds. Spitzy, K., Karrer, K. (H. Egermann, Vienna), Vol. 5, pp. 108/133–108/137 (abstr.).

‖Von Graevenitz, A., Bucher, C., Spitzy., K. H., Karrer, K. (1983) in *Proceedings of the 13th Internal Congress of Chemotherapy*, eds. Spitzy, K., Karrer, K. (H. Egermann, Vienna), Vol. 5, pp. 108/3–108/5 (abstr.).

**Schuster, I., Fleschurz, C., Hildebrandt, J., Turnowsky, F., Zsutty, H., Kretschmer, G., Spitzy, K. H., Karrer, K. (1983) in *Proceedings of the 13th Internal Congress of Chemotherapy*, eds. Spitzy, K., Karrer, K. (H. Egermann, Vienna), Vol. 5, pp. 108/42–108/46 (abstr.).

††Ganzinger, U., Stephen, A., Obenaus, H., Baumgartner, R., Walzl, H., Brueggemann, S., Schmid, B., Racine, R., Schatz, F., Haberl, H., *et al.* (1983) in *Proceedings of the 13th Internal Congress of Chemotherapy*, eds. Spitzy, K., Karrer, K. (H. Egermann, Vienna), Vol. 5, pp. 108/53–108/57 (abstr.).

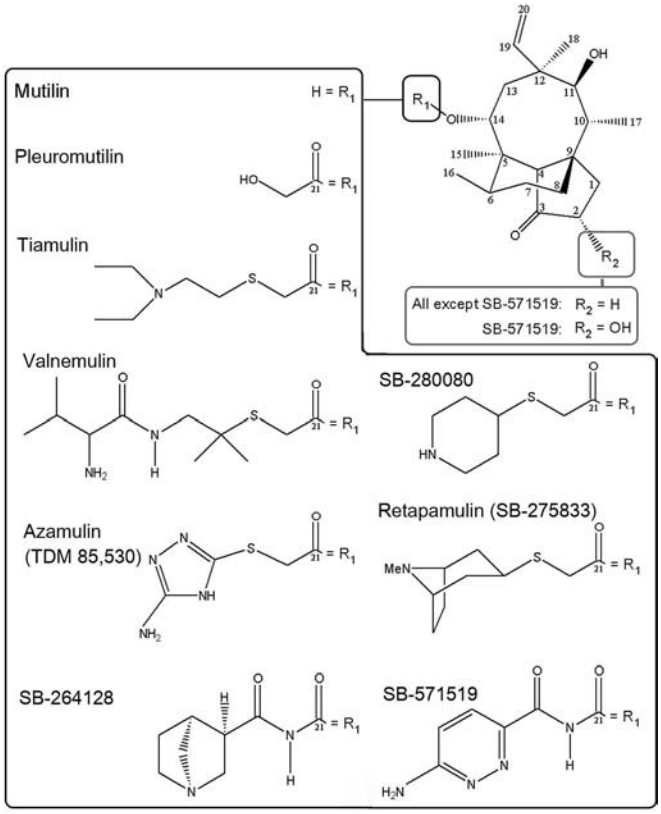

Fig. 1. Chemical formula of selected pleuromutilin derivatives. Typically, the tricyclic mutilin core is conserved among pleuromutilin derivatives. Notable is the variability of the C14 extension (R_1 in the large box). Large box, previously studied pleuromutilins (*Left*); pleuromutilins characterized in the current study (*Right*); mutilin and the natural pleuromutilin (*Upper Left*); acyl-carbamate semisynthetic derivatives (*Lower*). Notable is the conserved C21 carbonyl that is crucial for pleuromutilins activity (3, 16). (*Upper Right*) Small box, R_2, the acyl-carbamate derivative SB-571519 includes an additional hydroxyl that substituted on C2.

isons between the structures of these three complexes, the structure of native D50S and of its complex with tiamulin led to the discovery of a mechanism for their activity, and revealed the principles underlining their selectivity and their modes of action.

Results

Complete crystallographic data sets of complexes of D50S with SB-571519, SB-280080, and retapamulin (SB-275833) yielded electron density maps at 3.50, 3.56, and 3.66-Å resolution, respectively (Table 1), in which the location and conformation of each of the three bound compounds were unambiguously resolved (Fig. 2). Grouped occupancy refinement yielded a value of ≈1.0 for all three compounds, confirming that the they are quantitatively bound, in accord with the high binding affinity observed (Table 2) in a competitive ribosome-binding assay by using a radiolabeled pleuromutilin derivative (21).

The electron density maps of all three pleuromutilins complexes (Fig. 2 *a–c*) indicate that each of the pleuromutilins are located at the PTC, as in tiamulin (22), in the vicinity of the location that should have been occupied by the transition state intermediate of peptide bond formation (23). Their tricyclic cores are oriented similar to that observed for tiamulin (Fig. 3) and interact with the 23S RNA domain V (Fig. 2 *d–f*) by hydrophobic interactions and hydrogen bonds, formed mainly with surrounding nucleotides, namely A2503, U2504, G2505, U2506, C2452, and U2585. The C11 hydroxyl group of all of the compounds is located in a position suitable for hydrogen bonding to G2505 phosphate, as previously observed for tiamulin. In SB-280080 and SB-571519, it can be involved in an additional H-bond with the O2′ hydroxyl of A2503 (Fig. 2 *d* and *f*). The additional hydroxyl group of SB-571519 C2 (R_2 in Fig. 1) may be involved in polar interactions or an H-bond with O3′ or O5′ phosphoester of G2505 (Fig. 2*d*), because the distances between its oxygen and G2505 phosphoester oxygens are 3.2 and 3.0 Å, respectively.

As observed for tiamulin (22), the essential (3) C21 keto group (Fig. 1) of the C14 extension of all three compounds is involved in two to three hydrogen bonds with G2061. This H-bond network is similar for all three compounds, including the carbamate derivative SB-571519 that utilizes its additional carbonyl as an alternative H-bond acceptor (Fig. 2 *d–f*). Apart from these H-bonds with G2061, it seems that the pleuromutilins' C14 extension is involved only in minor hydrophobic contacts with ribosomal nucleotides.

Among the conformational rearrangements of the rRNA observed upon binding of all three studied pleuromutilins (Fig. 2 *g–i*), the most notable is the 40° rotation of U2506 base toward the tricyclic core, a motion that closes tightly the binding pocket on the bound compound. An additional conformational rearrangement, of the flexible base of U2585 (24, 25), was also detected. In eubacteria, in the absence of substrates or inhibitors, this flexible nucleotide (26) is located in a position (27–29) that should interfere or interact with C14 extension of all studied pleuromutilins, including tiamulin. Consequently, to avoid steric hindrance, in the presence of pleuromutilins U2585 undergoes a slight shift, which allows for interactions between its base and that of U2506, thus stabilizing the conformations of both nucleotides in the bound state (Fig. 2 *d–f*). In the SB-571519- and SB-280080-bound forms, U2585 forms a single hydrogen bond with U2506, whereas in the retapamulin complex the distance between the two bases allows for van der Waals or similar interactions.

It was previously suggested that mutations in ribosomal protein L3 reduce bacterial susceptibility to pleuromutilins by indirect influence of the binding pocket conformation (22, 30, 31). Unambiguous tracing of protein L3 Arg-144 could be performed owing to the high quality of the electron density map of SB-571519 complex, as it was constructed from a complete dataset collected form a single crystal with significant redundancy (Table 1), showed that it extends toward the PTC, and interacts electrostatically with U2506 phosphate, but does not make any contacts with the pleuromutilin compound (Fig. 4*a*). In addition, no significant conformational rearrangements were detected in protein L3 in case of all studied pleuromutilin derivatives as well as tiamulin (22).

Discussion

Induced-Fit Mechanism for Pleuromutilin Binding. U2506 and U2585 undergo the most significant rRNA structural rearrangements upon binding of all three pleuromutilins. The conformational alterations of U2506 tightly close the binding pocket on the bound tricyclic core of all pleuromutilins (Fig. 2 *g–i*). The altered conformation of U2506 is stabilized by its hydrophobic interactions with the bound compound as well as by its interactions with U2585, which shifts away from the C14 extension. These interactions may account for the protection of N3 in U2506 and U2585 on chemical footprinting by 1-cyclohexyl-3-(2-morpholinoethyl) carbodiimide metho-*p*-toluenesulfonate in *Escherichia coli* and *B. hyodysenteriae* in the presence of tiamulin, valnemulin, pleuromutilin, and the carbamate derivative SB-264128 (Fig. 1) (20, 30–32). It is worth noting that U2506 and U2585 motions are not conditional for pleuromutilins binding because slightly different location of the compound can partially compensate for it, as observed for tiamulin, an additional C14-sulfanyl acetate derivative (22).

U2506 and U2585 nucleotides were identified as essential for ribosomal function biochemically (33) and by systematic genetic selection (34). Both nucleotides are highly flexible, as shown by the differences of their orientations in crystals kept in environments

Table 1. Data statistics

Compound	SB-571519	SB-280080	Retapamulin (SB-275833)
Crystal information			
Space group	I222	I222	I222
a	170.4	170.5	170.1
b	405.8	412.7	405.9
c	703.8	696.7	695.2
Diffraction data statistics			
X-ray source	ID19, SBC/APS	ID19, SBC/APS	ID19, SBC/APS
Wavelength, Å	1.033201	0.97933757	0.979290
Number of crystals	1	7	9
Crystal oscillation	0.3°–0.8°	0.3°–0.4°	0.3°–0.5°
Resolution, Å	30–3.50 (3.62–3.50)	30–3.56 (3.69–3.56)	30–3.66 (3.79–3.66)
Unique reflections	284,085	263,433	243,598
Observed reflections	1,400,909	1,541,408	1,973,738
Redundancy	4.9 (4.1)	5.9 (3.2)	8.1 (3.7)
Completeness, %	92.7 (84.9)	90.7 (70.2)	93.1 (70.0)
$\langle I \rangle / \langle \sigma \rangle$	6.3 (1.5)	7.2 (1.5)	9.1 (1.4)
R-merge, %	18.4 (79.7)	16.8 (70.2)	19.0 (79.1)
Refinement			
R-factor, %	27.5	27.6	26.0
R-free (5%), %	33.4	33.8	33.4
rmsd bonds, Å	0.008	0.008	0.008
rmsd angles, °	1.4	1.4	1.4

that are close (27) or far (35) from physiological conditions. Consistently, conformational rearrangements of both nucleotides were observed in several crystal structures of complexes of the large ribosomal subunit with substrate analogs (36). In particular, U2585 flexibility was suggested to provide means for the 3′ end tRNA A- to P-site rotatory motion (26), for D-amino acid rejection (25), and for facilitating the synergistic action of the streptogramins (24). Hence, it appears that the binding of pleuromutilins utilizes the intrinsic flexibility of the ribosome, and thereby undergoes induced fit for binding of a large ensemble of compounds. Such an induced-fit mechanism is consistent with kinetic data showing a prolonged retapamulin off-rate from *S. aureus* ribosomes, as well as with data suggesting that retapamulin inhibits P-site substrate binding independently of substrate concentration (21).

C14 Extension Is Located in the PTC Void. In all cases, the C14 extension is located in the PTC and is held mainly by a two- to three–hydrogen-bond network between G2061 and the essential C21 keto of the bound compound (3). In addition, in all cases U2585 is shifted away from the bound compound, to allow pleuromutilins binding. However, although in its altered location U2585 is in close proximity to C14 extension, it does not interact with it (Fig. 2 *d–f*), regardless of the chemical nature of the C14 extension. The most prominent alteration of U2585 has been observed in the presence of the rigid C14 extension of SB-571519, where U2585 is shifted >3 Å away from its native conformation (Fig. 2*g*).

In all three cases, the C14 extensions are located at the PTC, between the locations of the acetylated and the peptidylated tRNA CCA ends (Fig. 3) (37). All amino acids, of varying chemical

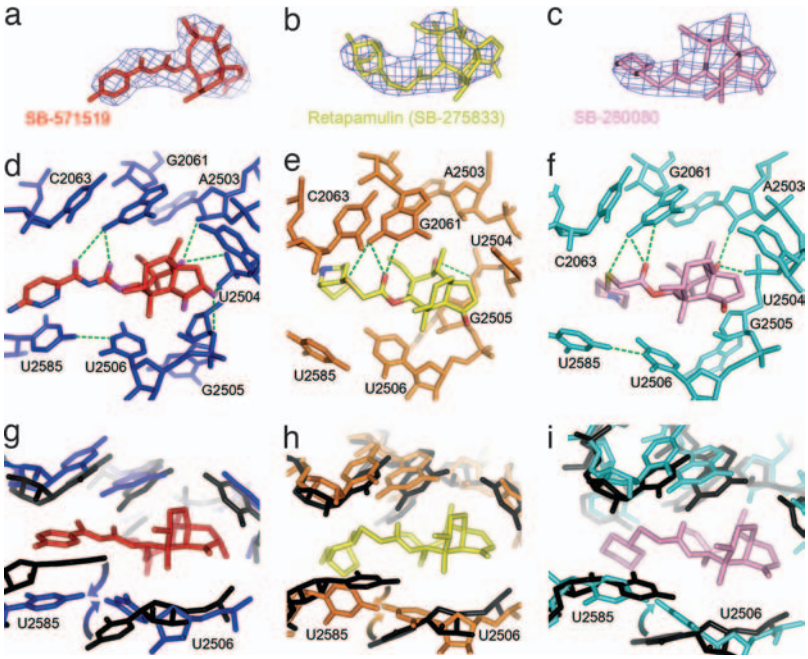

Fig. 2. Selected regions from the crystal structures of the large ribosomal subunit from *D. radiodurans* complexed with pleuromutilin acyl-carbamate derivative SB-571519 (in red: *a*, *d*, and *g*) and two sulfanyl-acetate derivatives retapamulin (SB-275833) (in yellow: *b*, *e*, and *h*) and SB-280080 (in pink: *c*, *f*, and *i*) at 3.50, 3.66, and 3.56-Å resolution, respectively. (*a–c*) $2F_o - F_c$ electron density maps, contoured at 1.5 σ level. (*d–f*) Interactions between pleuromutilin derivatives and 23S rRNA (the 23S rRNA bound conformation is shown in dark blue for SB-571519, orange for SB-275833, and cyan for SB-28008). All show H-bonds between G2061 and pleuromutilins' C14 extension and the possibility of H-bond between C11 hydroxyl and G2505 phosphate. In SB-571519 and SB-280080 complexes, C11 hydroxyl may serve as acceptor in an additional H-bond with the OH group of A2503 O2′, and a nontypical H-Bond is observed between U2585 and U2506. (*g–i*) Induced-fit mechanism promotes pleuromutilins binding (color code as in *d–f*). In all, the unbound 23S rRNA (PDB ID code 1NKW) is black, and the pleuromutilin-bound conformations are colored. On binding, U2585 translates away from the C14 extension and U2506 rotates toward the pleuromutilin and thus closes tightly the binding pocket. H-bonds (*d* and *f*) or other interactions (*e*) between the two shifted nucleotides may further stabilize the rRNA conformation at the bound state.

BIOCHEMISTRY

Table 2. Affinities of pleuromutilin derivatives in binding to *E. coli* ribosomes

Compound	K_d, nM
SB-275833	2.0 ± 0.05
SB-280080	7.5 ± 1.4
SB-571519	11.1 ± 3.2

Values are results ± standard error from two independent experiments.

characteristics, can be equally accommodated in this space. As this region contain only a few candidates for interactions, by its nature it should tolerate binding of various chemical moieties (38). This explains why all C14 extensions of the bound compounds hardly interact with PTC components. Instead, longer extensions may interact with distal rRNA nucleotides, as observed crystallographically for tiamulin (22) or suggested, based on biochemical evidences, for valnemulin (37). The small number of interactions of the C14 extensions rationalizes the similar activity of the different C14 pleuromutilin derivatives (39) and permits more flexibility in the design of this moiety.

Comparing the present findings with previous results (3, 16, 21) indicated that conditional to pleuromutilins activity is the H-bond network of C14 with G2061. Of importance is the C21 carbonyl group (Fig. 1) that exists also in the pleuromutilin mother compound and forms an H-bond with G2061 in all of the structurally studied pleuromutilins. Consistently, attempts to eliminate this group resulted in significantly lower or no activity (3, 16). An example for a successful modification of C14 extension is the C14-acyl-carbamate pleuromutilin derivatives, here represented by SB-571519. The slightly decreased binding affinity of the acyl-carbamate derivative in comparison to the sulfanyl-carbamate derivatives (Table 2) may result from less optimal H-bond formed by the rigid acyl-carbamate group with G2061. This may lead to a slightly lower affinity of SB-571519 in respect to the studied sulfanyl acetate derivatives (Table 2). Importantly, it was shown that this slight decrease in activity can be tolerated clinically, in view of the low metabolism rates of the acyl-carbamates (15, 16) compared with the C14-sulfanyl-acetate derivatives, which are rapidly eliminated by cytochrome P450.**

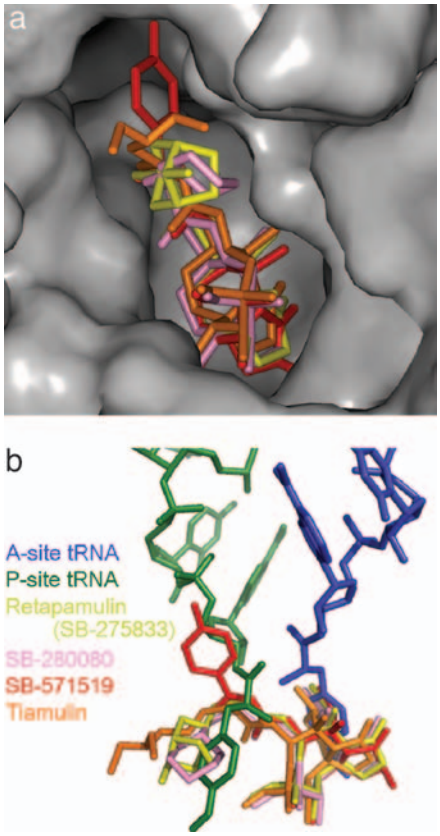

Fig. 3. Four pleuromutilin derivatives superimposed in the binding pocket. (*a*) A surface representation of the binding pocket. Several nucleotides have been removed to permit a clear view of the binding site. The structure of D50S/SB-517519 was used for surface representation. (*b*) A side view of pleuromutilins with the 3′ ends of an A-site tRNA mimic and the derived P-site tRNA (31). All pleuromutilin derivatives presented here are located at the PTC, with their tricyclic core oriented similar to tiamulin (22) and their C14 extensions placed within the PTC.

Pleuromutilin Resistance. The slow stepwise manner of the appearance of pleuromutilin resistance is consistent with the finding that several pleuromutilin resistant strains include more than one mutation (31). Furthermore, the majority of the nucleotides that are mutated for acquiring resistance do not directly interact with the bound compound, consistent with the essentiality of the interacting nucleotides for ribosomal function. It appears, therefore, that the strategy for acquiring resistance to antibiotics targeting the vicinity of the PTC is mutating nonconserved ribosomal components that do not belong to the essential portion of the PTC, but are involved in an interaction network with PTC nucleotides in a manner crucial for the organization of its functional conformation. Thus, it appears that these mutations reshape the conformation of this region, and/or alter its functional flexibility, in a fashion similar to allosteric rearrangements.

Likewise, the nonconserved region of L3 protein, residing in the vicinity of the PTC highly conserved nucleotides, enables such mechanism by mediating fine tuning of the PTC key nucleotides. The crystal structures of ribosome bound pleuromutilins presented here confirm that the majority of pleuromutilin-rRNA interactions are between the tricyclic core and the binding pocket, and that most of these contacts are formed regardless of the chemical nature of their C14 extension (Fig. 2 *d–f*). Furthermore, the addition of hydroxyl group at C2 in SB-571519 did not result in remarkably different binding orientation. Hence, it is not surprising that many pleuromutilin resistance mutations, identified in animal pathogens, involve nucleotides residing in the vicinity of the mutilin core, namely G2032, C2055, G2447, C2499, A2572, and U2504 (31). A similar effect has been previously observed for several mutations in the nearby protein L3.

Although different in sequence, in all known structures of the large ribosomal subunit (27–40) protein L3 penetrates deeply toward the PTC (Fig. 4 *a–c*). Several mutations that cluster in a loop-like region of L3 at the proximity of the PTC induce resistance or reduce susceptibility to pleuromutilins (31) (Fig. 4*b*), presumably by altering the rRNA conformation or flexibility in the vicinity of the binding site (22, 30). Similar resistance mechanisms were observed in yeasts (41, 42), where mutations in the corresponding L3 residues 255 to 257 (43) are responsible for anisomycin resistance.

In D50S/SB-571519 complex, Arg-144 of L3 interacts electrostatically with the phosphate of U2506 (Fig. 4*a*), a nucleotide playing a key role in pleuromutilin binding, thus showing that this L3 region is capable of interacting with PTC nucleotides involved in pleuromutilin binding. These particular electrostatic interactions may be specific to *D. radiodurans*, as the entire 6-aa loop-like region of L3 hosting Arg-144 displays a rather high sequence diversity (Fig. 4*b*). Nevertheless, the principle of reshaping a functional region composed of highly conserve nucleotides by using a nonconserve protein segment, is likely to be of a general character.

Pleuromutilin Selectivity Acquired by Remote Interactions. The key for clinical usage of antibiotics is their selectivity, namely the distinction between pathogens and their eukaryotic hosts. As the

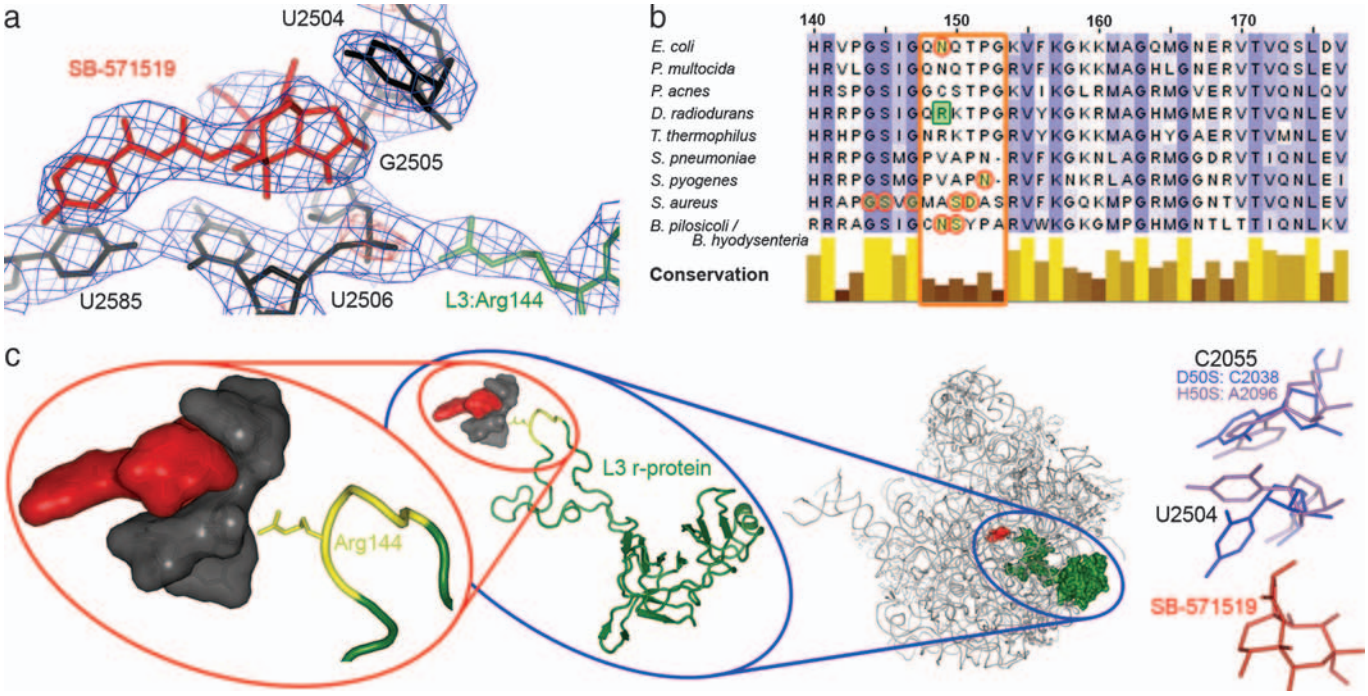

Fig. 4. Remote factors acquiring resistance and selectivity. (*a–c*) Possible contribution of L3 to pleuromutilin resistance. (*a*) 2 $F_o - F_c$ electron density map of the carbamate-derivative (red) SB-571519. 23S rRNA nucleotides are shown in black, and protein L3 Arg144 in green. Blue mesh is contoured at 1.0σ. The red meshes (contoured at 5.0σ) indicate phosphate locations. (*b*) Multiple sequence alignment of protein L3 from selected bacteria. Top numbering according to *E. coli* (where Arg144 of *D. radiodurans* is Asn149), bottom bars indicate conservation among these strains, and yellow circles indicate mutations with reduced pleuromutilin susceptibility in *E. coli* (30), *S. pyogenes*, *S. aureus* (12), *B. pilosicoli*, and *B. hyodysenteriae* (31). Most of these mutations are located in a highly diverse 6-aa window (orange box). In *D. radiodurans*, this window includes Arg144 (green square). (*c*) L3 protein penetrate from the surface of the ribosome deeply toward the vicinity of the PTC (right image, L3 in green, SB-571519 in red). The L3 nonconserve loop-like region (consisting of six amino acids, shown in *b* in the orange box) is colored yellow in the center and left image. In *D. radiodurans*, Arg144 electrostatically interacts with U2506 phosphate (*a*). 23S rRNA nucleotides 2504 to 2506 (left, gray surface representation) define a large portion of induced-fit binding pocket, obtained mainly by conformational change of U2506 (see Fig. 2 *g–i* and *Induced-Fit Mechanism for Pleuromutilin Binding*). (*d*) Differences in remote nucleotides acquire pleuromutilin selectivity. An example is U2504, which is among the nucleotides that define pleuromutilins binding site. In eubacteria it points toward the PTC, whereas in the Archaeon H50S, this nucleotide stacks with 2055, which is A in eukarya and archaea but C in eubacteria. This stacking seems to stabilize U2504 position away from the binding pocket. SB-571519 is red; nucleotides 2504 and 2055 are blue in its complex with D50S and purple in H50S.

pleuromutilins bind to the highly or universally conserved PTC nucleotides (44), their selectivity is attributed to differences in the boundaries of the binding pocket induced by the non conserved nucleotides residing in its vicinity. Thus, pleuromutilins seem to discriminate between eubacteria and higher organisms in a fashion similar to that used for acquiring resistance, exploiting interactions between nucleotides that do not interact with the bound compounds, in a manner resembling allosteric effects.

An example for kingdom-related differences in the orientation of a major element in the binding pocket is nucleotide U2504. In the structure of the eubacterial large ribosomal subunit from *D. radiodurans* (27), in its complex with pleuromutilin (22), and in eubacterial *E. coli* ribosome (28), this nucleotide points into the pleuromutilin binding pocket (Fig. 4*d*), whereas in the large ribosomal subunit of the Archaeon *Haloarcula marismortui*, H50S (35) this nucleotide is tilted away from the binding site, presumably owing to its interactions with C2055. The difference in the identity of this nucleotide, namely cytosine in eubacteria but adenine in archaea (>80%) and eukarya (>96%) (44) seems to indirectly alter the binding site conformation, and consequently the affinity of pleuromutilins. In support of this hypothesis is the C2055A mutation that decreases the susceptibility of *Brachyspira* species to pleuromutilins (31). An additional component that may promote drug discrimination is the significant sequence variability of protein L3 loop-like region that may trigger rRNA conformational differences among the pleuromutilin-binding pocket of ribosomes from different species.

Conclusions

Our studies revealed an induced-fit mechanism to promote tight binding, hinging on using its inherent flexibility and allowing for the rotational motion of a specific nucleotide, U2506. Interestingly, the dynamic properties of this nucleotide that seem to play a key role in ribosomal function are exploited for enhancing the tightness of the binding of ribosome inhibitors, the pleuromutilins. Thus, on pleuromutilin binding, the motion of U2506 closes the binding pocket on the bound mutilin core, which is involved in most of its interactions with its binding pocket.

An interaction network around the ribosome active site, which plays a key role in preserving its active conformation and allowing for its inherent functional flexibility, has been identified by investigating the modes of pleuromutilins binding to the eubacterial ribosome. Because all of the nucleotides that directly interact with the bound compounds are involved in peptide bond formation, therefore highly or universally conserved, they cannot contribute to selectivity. Likewise, these nucleotides are unlikely to undergo mutations. Consequently, resistance to pleuromutilins is acquired mainly by the mutations of less conserved nucleotides that do not interact with the bound compound, but can alter the surface of the binding pocket through remote interactions. Likewise, variability among species can be attributed to the PTC conformation. For example, the proximity of a loop-like region of protein L3 to pleuromutilin binding site, in the immediate vicinity of the PTC, may lead to diversity enabling fine tuning of rRNA conformation or flexibility without altering the PTC conserved nucleotides, hence contributing to the pleuromutilins selectivity.

The broad-spectrum activity of pleuromutilins and their unique binding site, the indications for maintaining slow resistance-development rates, and the relatively low cross-resistance with other clinical relevant antibiotics, explain why the prospects of using pleuromutilins as useful antibiotics are quite favorable. In particular, in all of the studied pleuromutilin complexes the C14 extension seems to interact mildly with ribosomal moieties, except for the common H-bonds network with G2061. This nonsticky nature of the C14 extension is advantageous for drug improvement, as it provides the basis for further drug modifications, designed to improve drug properties beyond the mere binding to the ribosome.

Materials and Methods

Crystallization and Data Collection. D50S crystals were obtained as previously described (45). Individual crystals were soaked in harvesting solution at room temperature with 0.01 mM retapamulin (SB-275833) or SB-280080 for 12 h, or 0.1 mM SB-571519 for 8 h and then transferred into freezing solution (45) for 10 min in the presence of the pleuromutilins. This was followed by flash freezing in liquid nitrogen. X-ray diffraction data were collected at 85 K. A few crystals were needed to yield complete datasets of D50S complexes with SB-275833 and SB-280080. However, a complete set with significant redundancy could be collected from a single crystal of the SB-571519 complex (Table 1).

Data Processing, Structure Solution, and Refinement. Data processed with HKL2000 (46) and CCP4 package suite (47). The pleuromutilin derivatives binding sites were unambiguously located in sigmaa-weighted difference electron density maps by using the native structure of D50S (PDB ID code 1NKW) as reference, after refinement by CNS (48). Because no crystal structure of any isolated pleuromutilin derivative is available, initial models were generated from tiamulin coordinates (PDB ID code 1XBP) modified by using insight II (Accelrys, San Diego, CA) and CORINA (www.molecular-networks.com/software/category/gen3dcoord.html), followed by energy minimization with no x-ray terms. The maps were traced interactively by using O (49) and COOT (50), followed by subsequent restraint CNS minimization for the entire complex. The same randomly selected 5% of the data were omitted for cross validation of all refinement procedures. The resulting coordinates have been deposited at the Protein Data Bank with PDB ID codes 2OGM, 2OGN, and 2OGO.

Numbering, Sequence Alignment, and Images. Nucleotides are numbered according to *E. coli* numbering system throughout, unless otherwise mentioned. For the L3 protein, the numbering is according to *D. radiodurans* because of the large sequence variability among different species. L3 multiple sequence alignment was performed by ClustalW (51) and presented by JalView (52). Figures were generated by Pymol (53).

K_d Determination of Pleuromutilin-Binding to *E. coli* Ribosomes. A radioligand displacement assay using [^{3}H]SB-258781 was used to determine the affinity of SB-571519, SB-280080, and SB-275833 to *E. coli* ribosomes (21). The binding data were fit to a cubic equation (GraFit; Erithacus Software Ltd., Surrey, U.K.) that solves K_d for a single binding site with two competitive ligands (54).

We thank Drs. Kang Yan and Robert A. Copeland for providing analytical procedures and for critical guidance in analyzed the data, Eric Hunt and Benjamin Bax for their constant stimulation and valuable discussions, and all members of the ribosome group at The Weizmann Institute for participating in the actual experimental work and for illuminating discussions. X-ray diffraction data were collected at Beamline 19ID of the Structural Biology Center at the Advanced Photon Source at Argonne National Laboratory and at Beamline ID14-4 of the European Synchrotron Radiation Facility–European Molecular Biology Laboratory. Funds were provided by the National Institutes of Health Grant GM34360 (to A.Y.) and by the Kimmelman Center for Macromolecular Assemblies (to A.Y.). The supplementary biochemical studies were funded by GlaxoSmithKline (to R.R.G.). A.Y. holds the Martin and Helen Kimmel Professorial Chair.

1. Diekema DJ, BootsMiller BJ, Vaughn TE, Woolson RF, Yankey JW, Ernst EJ, Flach SD, Ward MM, Franciscus CL, Pfaller MA, *et al.* (2004) *Clin Infect Dis* 38:78–85.
2. Kavanagh F, Hervey A, Robbins WJ (1951) *Proc Natl Acad Sci USA* 37:570–574.
3. Egger H, Reinshagen H (1976) *J Antibiot (Tokyo)* 29:923–927.
4. Berner H, Turnowsky F, Laber G, Hildebrandt J (1980) Eur Pat Appl EP0013768.
5. Rittenhouse S, Biswas S, Broskey S, McCloskey L, Moore T, Vasey S, West J, Zalacain M, Zonis R, Payne D (2006) *Antimicrob Agents Chemother* 50:3882–3885.
6. Rittenhouse S, Singley C, Hoover J, Page R, Payne D (2006) *Antimicrob Agents Chemother* 50:3886–3888.
7. Ross JE, Jones RN (2005) *J Clin Microbiol* 43:6212–6213.
8. Boyd B, Castaner J (2006) *Drugs Future* 31:107–113.
9. Goldstein EJ, Citron DM, Merriam CV, Warren YA, Tyrrell KL, Fernandez HT (2006) *Antimicrob Agents Chemother* 50:379–381.
10. Jones R, Fritsche T, Sader H, Ross J (2006) *Antimicrob Agents Chemother* 50:2583–2586.
11. Pankuch G, Lin G, Hoellman D, Good C, Jacobs M, Appelbaum P (2006) *Antimicrob Agents Chemother* 50:1727–1730.
12. Kosowska-Shick K, Clark C, Credito K, McGhee P, Dewasse B, Bogdanovich T, Appelbaum PC (2006) *Antimicrob Agents Chemother* 50:765–769.
13. Parish LC, Jorizzo JL, Breton JJ, Hirman JW, Scangarella NE, Shawar RM, White SM; SB275833/032 Study Team (2006) *J Amer Acad Dermatol* 55:1003–1013.
14. Free A, Roth E, Dalessandro M, Hiram J, Scangarella N, Shawar R, White S; SB275833/030 Study Group (2006) *Skinmed* 5:224–232.
15. Hunt E (2000) *Drugs Future* 25:1163–1168.
16. Brooks G, Burgess W, Colthurst D, Hinks JD, Hunt E, Pearson MJ, Shea B, Takle AK, Wilson JM, Woodnutt G (2001) *Bioorg Med Chem* 9:1221–1231.
17. Hodgin LA, Hogenauer G (1974) *Eur J Biochem* 47:527–533.
18. Hoegenauer G (1974) *Topics Infect Dis* 1:235–244.
19. Dornhelm P, Hogenauer G (1978) *Eur J Biochem* 91:465.
20. Poulsen SM, Karlsson M, Johansson LB, Vester B (2001) *Mol Microbiol* 41:1091–1099.
21. Yan K, Madden L, Choudhry A, Voigt CS, Copeland RA, Gontarek RR (2006) *Antimicrob Agents Chemother* 50:3875–3881.
22. Schlunzen F, Pyetan E, Fucini P, Yonath A, Harms JM (2004) *Mol Microbiol* 54:1287–1294.
23. Gindulyte A, Bashan A, Agmon I, Massa L, Yonath A, Karle J (2006) *Proc Natl Acad Sci USA* 103:13327–13332.
24. Harms JM, Schlunzen F, Fucini P, Bartels H, Yonath A (2004) *BMC Biol* 2:4–10.
25. Agmon I, Amit M, Auerbach T, Bashan A, Baram D, Bartels H, Berisio R, Greenberg I, Harms J, Hansen HA, *et al.* (2004) *FEBS Lett* 567:20–26.
26. Bashan A, Agmon I, Zarivach R, Schluenzen F, Harms J, Berisio R, Bartels H, Franceschi F, Auerbach T, Hansen HAS, *et al.* (2003) *Mol Cell* 11:91–102.
27. Harms J, Schluenzen F, Zarivach R, Bashan A, Gat S, Agmon I, Bartels H, Franceschi F, Yonath A (2001) *Cell* 107:679–688.
28. Schuwirth BS, Borovinskaya MA, Hau CW, Zhang W, Vila-Sanjurjo A, Holton JM, Cate JH (2005) *Science* 310:827–834.
29. Selmer M, Dunham CM, Murphy FV, IV, Weixlbaumer A, Petry S, Kelley AC, Weir JR, Ramakrishnan V (2006) *Science* 313:1935–1942.
30. Bosling J, Poulsen SM, Vester B, Long KS (2003) *Antimicrob Agents Chemother* 47:2892–2896.
31. Pringle M, Poehlsgaard J, Vester B, Long K (2004) *Mol Microbiol* 54:1295.
32. Long KS, Hansen LH, Jakobsen L, Vester B (2006) *Antimicrob Agents Chemother* 50:1458–1462.
33. Youngman EM, Brunelle JL, Kochaniak AB, Green R (2004) *Cell* 117:589–599.
34. Hirabayashi N, Sato NS, Suzuki T (2006) *J Biol Chem* 281:17203–17211.
35. Ban N, Nissen P, Hansen J, Moore PB, Steitz TA (2000) *Science* 289:905–920.
36. Schmeing TM, Huang KS, Strobel SA, Steitz TA (2005) *Nature* 438:520–524.
37. Nissen P, Hansen J, Ban N, Moore PB, Steitz TA (2000) *Science* 289:920–930.
38. Yonath A (2003) *Biol Chem* 384:1411–1419.
39. Berry V, Dabbs S, Frydrych CH, Hunt E, Woodnutt G, Sanderson FD (1999) Patent number WO9921855.
40. Korostelev A, Trakhanov S, Laurberg M, Noller HF (2006) *Cell* 126:1065–1077.
41. Fried HM, Warner JR (1981) *Proc Natl Acad Sci USA* 78:238–242.
42. Jimenez A, Sanchez L, Vazquez D (1975) *Biochim Biophys Acta* 383:427–434.
43. Meskauskas A, Petrov AN, Dinman JD (2005) *Mol Cell Biol* 25:10863–10874.
44. Cannone JJ, Subramanian S, Schnare MN, Collett JR, D'Souza LM, Du Y, Feng B, Lin N, Madabusi LV, Muller KM, *et al.* (2002) *BMC Bioinformatics* 3:1–31.
45. Auerbach-Nevo T, Zarivach R, Peretz M, Yonath A (2005) *Acta Crystallogr D Biol Crystallogr* 61:713–719.
46. Otwinowski Z, Minor W (1997) *Methods in Enzymology*, ed Carter C, Sweet R (Academic, London), Vol 276A, pp 307–326.
47. Bailey S (1994) *Acta Crystallogr D Biol Crystallogr* 50:760–763.
48. Brunger AT, Adams PD, Clore GM, DeLano WL, Gros P, Grosse-Kunstleve RW, Jiang JS, Kuszewski J, Nilges M, Pannu NS, *et al.* (1998) *Acta Crystallogr D Biol Crystallogr* 54:905–921.
49. Jones TA, Zou JY, Cowan SW, Kjeldgaard M (1991) *Acta Crystallogr A* 47:110–119.
50. Emsley P, Cowtan K (2004) *Acta Crystallogr D Biol Crystallogr* 60:2126–2132.
51. Thompson JD, Higgins DG, Gibson TJ (1994) *Nucleic Acids Res* 22:4673–4680.
52. Clamp M, Cuff J, Searle SM, Barton GJ (2004) *Bioinformatics* 20:426–427.
53. DeLano WL (2002) *The PyMOL Molecular Graphics System* (De Lano Scientific, San Carlos, CA).
54. Yan K, Hunt E, Berge J, May E, Copeland RA, Gontarek RR (2005) *Antimicrob Agents Chemother* 49:3367–3372.